

# Stabilization and Destabilization of Semiflexible Polymers Induced by Spherical Confinement

Martin Marenz, Johannes Zierenberg,\* and Wolffhard Janke

*Institut für Theoretische Physik, Universität Leipzig, Postfach 100 920, 04009 Leipzig, Germany*

Spherical confinement can act either stabilizing or destabilizing on the collapsed state of a semiflexible polymer. General free-energy arguments suggest that the order of the unconstrained collapse transition is the distinguishing factor: First order implies stabilization, second order causes destabilization. We confirm this conjecture by Monte Carlo simulations of a coarse-grained model for semiflexible polymers whose chain stiffness tunes the transition order. The resulting physical picture is potentially relevant for other systems under strong confinement such as proteins and DNA.

Confinement is an important element in nature's bag of tricks. Its utilization ranges from chaperone-mediated protein folding [1, 2] and subsequent modulation of amyloid formation [3, 4], over DNA packing in a viral capsid and its translocation into a host cell [5–12], to entropic segregation [13–15]. Recent results include confinement-induced coexistence of coil and globule domains along a single DNA chain [16]. Moreover, the same trick may be exploited for practical applications, including confinement-induced miscibility in polymer blends [17], enhanced dispersion in nanoparticle-polymer blend films [18], filament growth in flexible confinement [19], for nanodevices and their fabrication [20–22], and (DNA) nanopore sequencing [23]. It is thus desirable to have a systematic approach to predict or even tailor the behavior of polymers under confinement.

Semiflexible polymers are a generic model class for a systematic study of the leading-order effect of confinement on structural properties and thermal responses in polymeric systems in general. For flexible self-avoiding polymers, theoretical scaling analyses of the free energy revealed that spherical confinement is qualitatively different from planar or cylindrical confinement [24]. This is confirmed by mean-field calculations for (semi)flexible polymers, predicting several scaling regimes of the confinement-induced change in free energy [25, 26]. For self-attracting theta polymers, a change in free energy leads to a change in the collapse transition temperature. Since confinement generically increases the free energy, it seems surprising that computer simulation of flexible polymers revealed a destabilizing shift in the collapse temperature [27, 28], whereas simulations of semiflexible polymers revealed a stabilizing shift [27]. The latter is consistent with the trend in computational studies of proteins [29–33], which can be considered as a special (complex) class of rather rigid semiflexible polymers. However, adding solvent may change the stabilizing nature of confinement in this case [34].

In this Letter, we show that stabilization or destabilization of polymers, induced by a steric spherical confinement, is determined by the type of the free polymer collapse transition, being either first- or second-order. The relation to the stiffness of self-attracting semiflexible

polymers, exhibiting a rich structural phase space [35–37], is straightforward: For flexible polymers the collapse transition from an extended coil to a globule is known to be a continuous (second-order) transition, while for stiffer polymers the collapse (or folding) transition from rather stiff rods into bend linear strands, toroids, or hairpin structures, can be thought of as a discontinuous (first-order) transition [37]. In order to obtain general results, we combine free-energy arguments in the limit of infinite chain length with numeric results for coarse-grained polymers representing biologically more realistic finite chains. Altogether, this allows us to identify the order of the free-polymer collapse transition as the distinguishing factor for the stabilization or destabilization upon strong confinement.

To get a deeper understanding of the basic mechanism, we neglect the chemical details of complex macromolecules and consider a generic semiflexible homopolymer model that describes an entire class of semiflexible theta polymers. The homopolymer is modeled as a linear chain of  $N$  monomers connected by stiff bonds of length  $\sigma$ . Non-bonded monomers interact via the 12-6 Lennard-Jones potential

$$V_{\text{LJ}}(r_{ij}) = 4\epsilon \left[ \left( \frac{\sigma}{r_{ij}} \right)^{12} - \left( \frac{\sigma}{r_{ij}} \right)^6 \right], \quad (1)$$

where  $r_{ij}$  is the distance between two monomers,  $\epsilon = 1$  sets the temperature scale, and  $\sigma = 1$  sets the length scale. This models self-avoidance and short-range attraction leading to a thermally driven collapse transition. In addition, semiflexibility is modeled by the worm-like chain motivated bending potential

$$V_{\text{bend}}(\theta_i) = \kappa(1 - \cos \theta_i), \quad (2)$$

where  $\theta_i$  is the angle between adjacent bonds and  $\kappa$  is the stiffness parameter. The polymer is confined to a steric sphere of radius  $R$  with non-elastic repulsion at the shell.

Canonical equilibrium estimates are obtained from histogram reweighting [38] of replica-exchange Monte Carlo simulations [39] in the entire two-dimensional temperature-stiffness plane [36]. Each parallel instance samples with the Boltzmann weight  $\exp(-\beta E_{\text{LJ}} - \beta \kappa E_{\text{bend}})$ , where  $\beta = 1/k_{\text{B}}T$  is the inverse temperature with Boltzmann constant  $k_{\text{B}}$ ,  $E_{\text{LJ}} =$

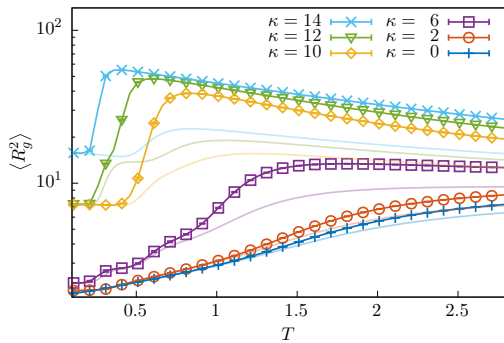
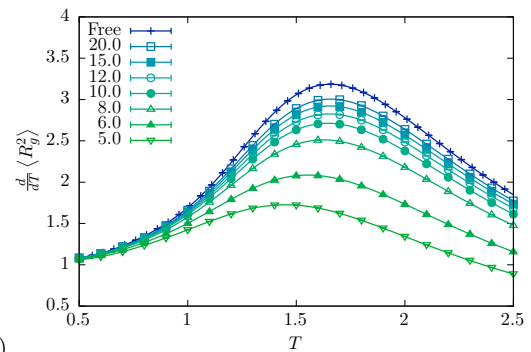


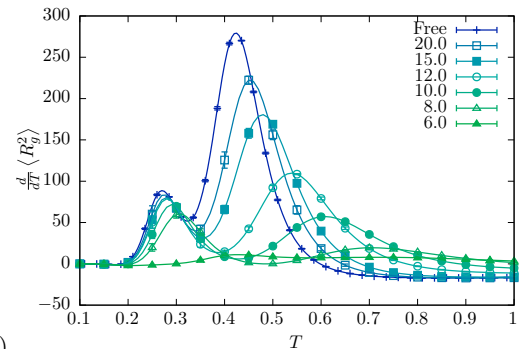
FIG. 1. Canonical equilibrium extension of a single semiflexible polymer of length  $N = 28$  estimated as the squared radius of gyration  $\langle R_g^2 \rangle$  for different  $\kappa$ . Intense lines with error bars show the unconfined case and opaque lines show the behavior in a sphere of radius  $R = 8$ .

$\sum_{i=1}^{N-2} \sum_{j=i+2}^N V_{\text{LJ}}(r_{ij})$  and  $E_{\text{bend}} = \sum_i^{N-2} V_{\text{bend}}(\theta_i)$ . In regular intervals replicas exchange their conformations according to the Boltzmann weights (see, e.g., Ref. [36] for details). We validated our data for the free case with estimates from parallelized multicanonical simulations [40–42]. In the scaling part, we restrict ourselves to the one-dimensional replica-exchange approach at fixed  $\kappa$ . A comprehensive overview is obtained for polymers of length  $N = 28$ , where we sampled the entire semiflexible range  $\kappa \in [0, 20]$  in the temperature interval  $T \in [0.1, 3.0]$  for sphere radii  $R \in \{5, 6, 8, 10, 12, 15, 20\}$ . To obtain the scaling exponents, we selected integer  $\kappa$  values and increased the number of sphere radii  $R \in [5, 120]$  until we obtained a clear result. We repeated this for shorter ( $N = 14$ ) and longer ( $N = 42$  and for  $\kappa = 0$  also  $N = 64$ ) chains. Error estimates are obtained with the Jackknife method [43].

We begin the discussion of our results by commenting on the effect of stiffness on the equilibrium collapse transition of a free theta polymer. Figure 1 shows a measure of the polymer extension – the squared radius of gyration  $R_g^2 = \sum_{i=1}^N (r_i - r_{\text{cm}})^2 / N$ , where  $r_{\text{cm}}$  is the center of mass. The free case is shown as intense colored curves, where lines are high-resolution estimates from histogram reweighting and error bars are shown for some selected points. For rather flexible polymers, we observe the expected second-order transition: At high temperatures the polymer is in an extended conformation (random coil) and, upon temperature decrease, continuously contracts to a globular equilibrium state. In this regime the bending energy is a subleading contribution and the problem reduces to the competition of maximizing conformational entropy by polymer extension and energy minimization by forming a compact structure. In contrast, for stiffer polymers we observe a first-order transition: At high temperatures the polymer is again in an extended conformation (at infinite temperature again random coil).



(a)



(b)

FIG. 2. Canonical thermal derivative of the squared radius of gyration  $\frac{d}{dT} \langle R_g^2 \rangle$  of a single semiflexible polymer ( $N = 28$ ) in spherical confinement of different radius  $R$ . Depending on the stiffness, the confinement induces destabilization shifting the transition to lower temperatures, e.g., for  $\kappa = 0$  in (a), or induces stabilization shifting the transition to higher temperatures, e.g., for  $\kappa = 12$  in (b).

Upon temperature decrease, the polymer initially stiffens and extends further towards a stiff rod until a point where it suddenly folds into more compact conformations such as hairpins or multiple linear strands [35–37]. The sudden decrease hints towards a (finite-size) “phase coexistence”, where the minimization of Lennard-Jones energy of compact states competes with the minimization of bending energy of relatively stiff rod-like chain strands.

The effect of confinement on the canonical estimates of  $R_g^2$  can be seen in Fig. 1 as opaque lines for the same polymer but in a steric sphere of small radius. This is here presented for  $N = 28$  but is qualitatively similar for shorter ( $N = 14$ ) and longer ( $N = 42$ ) chains. The single polymer may no longer be fully extended and we observe a decrease in  $\langle R_g^2 \rangle$  at high temperatures for all stiffnesses. The effect increases with stiffness because the extension of the free polymer increases with stiffness. As one may expect, the low-temperature behavior is barely influenced by the confinement. Depending on the stiffness, the confinement leads to two different modifications of the collapse transition:

For the case of flexible polymers, the confinement results in a gradual decrease of the polymer extension along the high-temperature regime which extends over

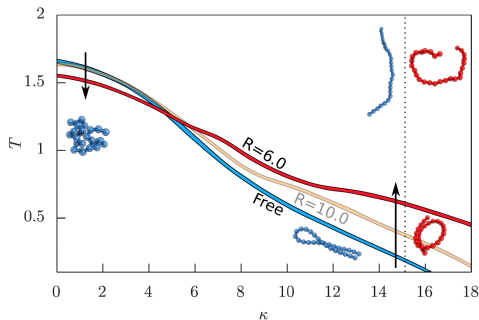


FIG. 3. Illustration of the stabilizing and destabilizing effect induced by spherical confinement on a semiflexible polymer (here  $N = 28$ ). Colors encode the size of confinement: free (blue),  $R = 10$  (orange), and  $R = 6$  (red). For flexible polymers, the collapse transition temperature decreases upon confinement thus destabilizing the collapsed state. For stiffer polymers, confinement increases the collapse transition temperature thus stabilizing the folded state. This may alter a hairpin structure into a purely toroidal state. For intermediate stiffness there is a crossover where confinement practically does not alter the transition. Exemplary conformations are shown in the color of the respective confinement strength at low stiffness ( $\kappa = 0.3$ ) and at large stiffness ( $\kappa = 15$ , marked by the dashed line).

the transition itself. As a result, the maximal slope here shifts to lower temperatures. This is further elucidated for the fully flexible polymer in Fig. 2 (a), showing that the peak of the thermal derivative of  $\langle R_g^2 \rangle$  shifts to *lower* temperatures with decreasing radius of the confining sphere.

The situation changes for more rigid polymers, where the spherical confinement strongly reduces the conformational entropy of only the high-temperature regime and forces the relatively stiff rods to exhibit a curvature that deviates from their free counterpart. This appears to be similar to the renormalization of persistence length known from steric disorder [44]. Figure 2 (b) shows the thermal derivative of  $\langle R_g^2 \rangle$  for a stiffer polymer, demonstrating that a decreasing confining sphere shifts the peak to *higher* temperatures. Notice that the lower-temperature peak already shows the next structural transition (“freezing”), which is only slightly influenced by the spherical confinement [28].

The qualitative behavior is summarized for the entire range of semiflexibility in Fig. 3. There is a general trend for flexible polymers to be destabilized by spherical confinement, i.e., the collapse transition temperature is reduced. For stiffer polymers, the transition temperature increases and the folded states are stabilized at higher temperatures. As for proteins, this may be accompanied by a change of the structural state, e.g., from hairpin to toroidal structures as shown in the figure. Similar structures have been observed recently for double-stranded

DNA in confinement [16], and as a result of DNA packing into viral capsids [5–9, 45]. We emphasize that the crossover from destabilization to stabilization ( $\kappa \approx 6$  for  $N = 28$ ) indeed roughly coincides with the crossover from a second-order to a first-order collapse transition in the free semiflexible polymer [37].

We now want to quantify our observations and provide general free-energy arguments from which one can deduce the direction and scaling form of the temperature shift from the type of free-polymer collapse transition. Let us begin with the first-order regime of stiffer polymers. At the transition, the collapsed regime is in coexistence with the extended regime. We can approximate this in a two-state model, where the system can only change between a structured state with free energy  $F_s$ , and an unstructured state with free energy  $F_u$ . Coexistence is then expressed in the relation  $e^{-\beta F_s} = e^{-\beta F_u}$  or  $0 = \beta F_u - \beta F_s$ . The spherical confinement predominantly affects the unstructured regime, decreasing the available entropy (and even increasing the accessible energy) which increases the free energy  $F_u = F_u^\infty + \Delta F \geq F_u^\infty$ , while  $F_s \approx F_s^\infty$ . We consider the temperature-independent correction ansatz  $\beta \Delta F = aR^{-\gamma}$  ( $a > 0$ ) in the unstructured (high-temperature) regime. This ansatz is consistent with all regimes found for semiflexible polymers in spherical confinement [26] and it yields

$$0 = \beta F_u^\infty - \beta F_s^\infty + aR^{-\gamma}. \quad (3)$$

We can estimate the (inverse) collapse temperature of the confined polymer,  $\beta_c(R) = 1/k_B T_c(R)$ , by a Taylor expansion around the free polymer collapse transition,  $\beta_c^\infty = 1/k_B T_c^\infty$ . Using  $\partial \beta F / \partial \beta = E$  and  $F_s^\infty(\beta_c^\infty) = F_u^\infty(\beta_c^\infty)$  yields

$$\beta_c(R) = \beta_c^\infty - aR^{-\gamma} / \Delta E^\infty. \quad (4)$$

In general, thermodynamics implies that  $\Delta E^\infty = E_u^\infty - E_s^\infty \geq 0$ , where equality may occur for topological transitions [36], in which case a higher-order expansion of (3) would be necessary. For the collapse transition of semiflexible polymers  $\Delta E^\infty > 0$  and we obtain a positive temperature shift

$$T_c(R) - T_c^\infty \propto R^{-\gamma} > 0. \quad (5)$$

The exponent depends on the free-energy excess that for semiflexible polymers shows several regimes [26], some of which are consistent with previous results for proteins where  $\gamma \approx 2 - 3$  [30]. Figure 4 shows that fits of Eq. (5) to our data for  $N = \{14, 28, 42\}$  indeed yield a stabilizing shift (blue symbols) in the high- $\kappa$  regime where  $\gamma$  is slightly increasing with  $\kappa$  in the range  $\gamma \approx 1 - 2$ .

Let us now turn to the second-order regime of flexible polymers. For a continuous transition, the confinement gradually increases the free energy at all temperatures, while the effect is of course higher at larger temperatures.

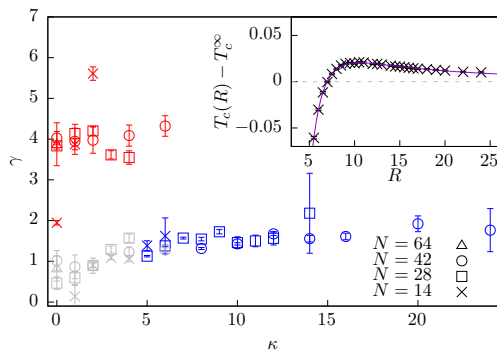


FIG. 4. Scaling exponent  $\gamma$  as a function of stiffness parameter  $\kappa$  for different  $N$ . For high  $\kappa$ , fits to Eq. (5) indicate stabilization (blue symbols,  $T_c(R) > T_c^\infty$ ) and  $\gamma(\kappa)$  shows a monotonic behavior. For low  $\kappa$ , fits to Eq. (7) show both subleading stabilizing (gray symbols,  $T_c(R) > T_c^\infty$ ) and dominant destabilizing (red symbols,  $T_c(R) < T_c^\infty$ ) contributions. An example of  $T_c(R) - T_c^\infty$  in the low- $\kappa$  regime at  $\kappa = 4$  is shown in the inset for  $N = 28$ .

A natural ansatz is to quantify the free-energy increase in terms of the dimensionless ratio of polymer extension and confinement size  $\beta\Delta F \sim (N^\nu/R)^x$ , where  $\nu$  is the Flory exponent with  $\nu \approx 3/5$  ( $\beta < \beta_c$ ),  $\nu = \nu_c = 1/2$  ( $\beta = \beta_c$ ), and  $\nu = 1/3$  ( $\beta > \beta_c$ ) in three dimensions. The ratio has to be extensive, i.e., for  $N \rightarrow aN$  we expect  $F \rightarrow aF$ , while  $R \rightarrow a^{1/d}R$ . It directly follows for flexible polymers in  $d$  dimensions that [25]

$$\beta\Delta F \sim \left(\frac{N^\nu}{R}\right)^{d/(d\nu-1)} = N \left(\frac{N}{R^d}\right)^{1/(d\nu-1)}. \quad (6)$$

In order to identify the confinement-induced shift of the collapse transition, we recall that for polymers of finite length the transition point is signaled by a shoulder in the specific heat  $C_V = -k_B\beta^2 \left[ \frac{\partial^2}{\partial\beta^2}(\beta F) + \frac{\partial^2}{\partial\beta^2}(\beta\Delta F) \right]$  [47]. The obvious temperature-dependent contribution to (6) is the step function  $\nu(\beta)$ , which for finite chains is rounded such that a linear expansion around the critical point yields  $\nu(\beta) \approx \nu_c - c(\beta - \beta_c)$  with  $c$  positive. We thus find that the confinement-induced change in specific heat scales as  $\Delta C_V \sim -k_B\beta^2 \left(\frac{N^\nu}{R}\right)^{\frac{d}{d\nu-1}} \left[ \frac{d^2c^2}{(d\nu-1)^4} \left(\ln \frac{N}{R^d}\right)^2 - \frac{2d^2c}{(d\nu-1)^3} \ln \frac{N}{R^d} \right]$ . This change is always negative and in the limit  $R \rightarrow \infty$  goes to zero because  $R$  grows faster than  $\ln R$ . Moreover, the change vanishes for  $\beta > \beta_c$  where  $\nu \rightarrow 1/3$  and is strongest for  $\beta < \beta_c$  where  $\nu \approx 3/5$ . Consequently, with decreasing  $R$  the shoulder in the specific heat moves to larger  $\beta$  (smaller  $T$ ) which destabilizes the collapse transition.

In the low- $\kappa$  regime of rather flexible polymers, our numerical results cannot be described by a single power-law scaling in  $R$ , see the inset of Fig. 4 for a typical example. For large  $R$ , the confinement initially weakly stabilizes the collapse transition, while destabilization eventually

happens for smaller  $R$ . With decreasing  $\kappa$ , the crossover radius increases and the size of the temperature shift decreases. Similar observations have been reported for polymers in slitlike confinement, where narrow slits increase the surface free energy of the globular state because more monomers are exposed to the surface [48]. For the present case, we thus make the extended ansatz

$$T_c(R) - T_c^\infty = a_1 R^{-\gamma_1} - a_2 R^{-\gamma_2}. \quad (7)$$

Indeed, the dominant shift in the low- $\kappa$  regime is destabilizing ( $a_2 \gg a_1$ ) with  $\gamma_2 \approx 4$  (Fig. 4, red symbols) in agreement with our predictions. For the special case of flexible polymers ( $\kappa = 0$ ), we find for small  $N$  a purely destabilizing effect ( $a_1 \approx 0$ ) with  $\gamma_2 = 1.95(5)$  ( $N = 14$ ), while for larger  $N$  again a combination of initial stabilization followed by a clear destabilization with  $\gamma_2 = 3.83(8)$  ( $N = 28$ ),  $\gamma_2 = 4.0(2)$  ( $N = 42$ ), and  $\gamma_2 = 3.9(5)$  ( $N = 64$ ). This is surprisingly consistent with the exponent of the confinement free-energy change, i.e.,  $\gamma_2 \approx d/(d\nu - 1) \approx 15/4 = 3.75$  (cf. Eq. (6)) of a flexible polymer [25, 28]. It is remarkable that the subdominant stabilization exponent (gray symbols) seems to extend the increasing trend of  $\gamma(\kappa)$  in the high- $\kappa$  regime, which is an interesting starting point for future investigation.

In summary, we have shown both stabilizing and destabilizing effects of spherical confinement on the entire class of generic semiflexible polymers. We highlight that using free-energy arguments we have identified the type of the free-polymer collapse transition as the distinguishing factor that governs the stabilizing (for first-order collapse) and destabilizing (for second-order collapse) response on spherical confinement. The type of transition in turn can be tuned in our generic model from second- to first-order by increasing the chain stiffness [37]. Our result relies on general free-energy arguments and should thus stay valid also for more complex polymers, proteins, and DNA. In fact, recent results on a special type of flexible polymers with a first-order collapse transition show a stabilizing shift in slitlike confinement [49].

Our results thus provide a simple explanation for the diverse results in the context of polymer collapse and protein folding upon confinement and it would be worthwhile to reassess the so far considered models in the presented framework. Moreover, our framework may serve as a guide to predict stabilization or destabilization induced by spherical confinement by studying whether the transition of a free macromolecule is first- or second-order. In fact, tailoring the transition behavior, e.g., by DNA origami [50] or by designing protein structures [51], should allow one to attain specific behavior under confinement. This may find application in targeted drug release or functionalization of macromolecules in specific confining environments.

We would like to thank Hannes Witt for stimulating discussions. This work was in part funded by the

European Union and the Free State of Saxony through the “Sächsische AufbauBank” and by the Deutsche Forschungsgemeinschaft (DFG) through SFB/TRR 102 (project B04) and Grant No. JA 483/31-1. Additional financial support was obtained by the Deutsch-Französische Hochschule (DFH-UFA) through the Doctoral College “L<sup>4</sup>” under Grant No. CDFA-02-07 and the Leipzig Graduate School of Natural Sciences “Build-MoNa”. The authors gratefully acknowledge the computing time provided by the John von Neumann Institute for Computing (NIC) on the supercomputer JURECA at Jülich Supercomputing Centre (JSC) under Grant No. HLZ24.

---

\* Current Address: Max Planck Institute for Dynamics and Self-Organization, Am Fassberg 17, 37077 Göttingen, Germany.

- [1] F. U. Hartl and M. Hayer-Hartl, *Molecular chaperones in the cytosol: From nascent chain to folded protein*, *Science* **295**, 1852 (2002).
- [2] J. C. Young, V. R. Agashe, K. Siegers, and F. U. Hartl, *Pathways of chaperone-mediated protein folding in the cytosol*, *Nat. Rev. Mol. Cell Biol.* **5**, 781 (2004).
- [3] F. U. Hartl, A. Bracher, and M. Hayer-Hartl, *Molecular chaperones in protein folding and proteostasis*, *Nature* **475**, 324 (2011).
- [4] P. Arosio, T. C. T. Michaels, S. Linse, C. Månsson, C. Emanuelsson, J. Presto, J. Johansson, M. Vendruscolo, C. M. Dobson, and T. P. J. Knowles, *Kinetic analysis reveals the diversity of microscopic mechanisms through which molecular chaperones suppress amyloid formation*, *Nat. Commun.* **7**, 10948 (2016).
- [5] J. Arsuaga, M. Vázquez, S. Trigueros, D. Witt Summers, and J. Roca, *Knotting probability of DNA molecules confined in restricted volumes: DNA knotting in phage capsids*, *Proc. Natl. Acad. Sci. USA* **99**, 5373 (2002).
- [6] J. Arsuaga, M. Vazquez, P. McGuirk, S. Trigueros, D. W. Summers, and J. Roca, *DNA knots reveal a chiral organization of DNA in phage capsids*, *Proc. Natl. Acad. Sci. USA* **102**, 9165 (2005).
- [7] C. Forrey and M. Muthukumar, *Langevin dynamics simulations of genome packing in bacteriophage*, *Biophys. J.* **91**, 25 (2006).
- [8] D. Reith, P. Cifra, A. Stasiak, and P. Virnau, *Effective stiffening of DNA due to nematic ordering causes DNA molecules packed in phage capsids to preferentially form torus knots*, *Nucl. Acids Res.* **40**, 5129 (2012).
- [9] Q. Cao and M. Bachmann, *Dynamics and limitations of spontaneous polyelectrolyte intrusion into a charged nanocavity*, *Phys. Rev. E* **90**, 060601 (2014); *Impact of surface charge density and motor force upon polyelectrolyte packaging in viral capsids*, *J. Polym. Sci. B Polym. Phys.* **54**, 1054 (2016).
- [10] A. Cacciuto and E. Luitjen, *Confinement-driven translocation of a flexible polymer*, *Phys. Rev. Lett.* **96**, 238104 (2006).
- [11] M. Muthukumar, *Mechanism of DNA transport through pores*, *Annu. Rev. Biophys.* **36**, 435 (2007).
- [12] Y. Hu, R. Zandi, A. Anavitarte, C. M. Knobler, and W. M. Gelbart, *Packaging of a polymer by a viral capsid: The interplay between polymer length and capsid size*, *Biophys. J.* **94**, 1428 (2008).
- [13] S. Jun and B. Mulder, *Entropy-driven spatial organization of highly confined polymers: Lessons for the bacterial chromosome*, *Proc. Natl. Acad. Sci. USA* **103**, 12388 (2006).
- [14] B.-Y. Ha and Y. Jung, *Polymers under confinement: Single polymers, how they interact, and as model chromosomes*, *Soft Matter* **11**, 2333 (2015).
- [15] A. Azari and K. K. Müller-Nedebock, *Entropic competition in polymeric systems under geometrical confinement*, *Europhys. Lett.* **110**, 68004 (2015).
- [16] B. Sung, A. Leforestier, and F. Livolant, *Coexistence of coil and globule domains within a single confined DNA chain*, *Nucl. Acids Res.* **44**, 1421 (2016).
- [17] S. Zhu, Y. Liu, M. H. Rafailovich, J. Sokolov, D. Gersappe, D. A. Winesett, and H. Ade, *Confinement-induced miscibility in polymer blends*, *Nature* **400**, 49 (1999).
- [18] S. Chandran, N. Begam, V. Padmanabhan, and J. K. Basu, *Confinement enhances dispersion in nanoparticle-polymer blend films*, *Nat. Commun.* **5**, 3697 (2014).
- [19] R. Vetter, F. K. Wittel, and H. J. Herrmann, *Morphogenesis of filaments growing in flexible confinements*, *Nat. Commun.* **5**, 4437 (2014).
- [20] Y. Wu, G. Cheng, K. Katsov, S. W. Sides, J. Wang, J. Tang, G. H. Fredrickson, M. Moskovits, and G. D. Stucky, *Composite mesostructures by nano-confinement*, *Nat. Mater.* **3**, 816 (2004).
- [21] M. M. A. E. Claessens, R. Tharmann, K. Kroy, and A. R. Bausch, *Microstructure and viscoelasticity of confined semiflexible polymer networks*, *Nat. Phys.* **2**, 186 (2006).
- [22] W. Reisner, J. N. Pedersen, and R. H. Austin, *DNA confinement in nanochannels: Physics and biological applications*, *Rep. Prog. Phys.* **75**, 106601 (2012).
- [23] D. Branton, D. W. Deamer, A. Marziali, H. Bayley, S. A. Benner, T. Butler, M. Di Ventra, S. Garaj, A. Hibbs, X. Huang, S. B. Jovanovich, P. S. Krstic, S. Lindsay, X. Sean Ling, C. H. Mastrangelo, A. Meller, J. S. Oliver, Y. V. Pershin, J. M. Ramsey, R. Riehn, G. V. Soni, V. Tabard-Cossa, M. Wanunu, M. Wiggins, and J. A. Schloss, *The potential and challenges of nanopore sequencing*, *Nat. Biotechnol.* **26**, 1146 (2008).
- [24] A. Cacciuto and E. Luitjen, *Self-avoiding flexible polymers under spherical confinement*, *Nano Lett.* **6**, 901 (2006).
- [25] T. Sakaue, and E. Raphaël, *Polymer chains in confined spaces and flow-injection problems: Some remarks*, *Macromolecules* **39**, 2621 (2006).
- [26] T. Sakaue, *Semiflexible polymer confined in closed spaces*, *Macromolecules* **40**, 5206 (2007).
- [27] Y. Higuchi, K. Yoshikawa, and T. Iwaki, *Confinement causes opposite effects on the folding transition of a single polymer chain depending on its stiffness*, *Phys. Rev. E* **84**, 021924 (2011).
- [28] M. Marenz, J. Zierenberg, H. Arkin, and W. Janke, *Simple flexible polymers in a spherical cage*, *Condens. Matter Phys.* **15**, 43008 (2012).
- [29] H.-X. Zhou and K. A. Dill, *Stabilization of proteins in confined spaces*, *Biochemistry* **40**, 11289 (2001).
- [30] F. Takagi, N. Koga, and S. Takada, *How protein thermodynamics and folding mechanisms are altered by the chaperonin cage: Molecular simulations*, *Proc. Natl. Acad. Sci. USA* **100**, 11367 (2003).

- [31] N. Rathore, T. A. Knotts IV, and J. J. de Pablo, *Confinement effects on the thermodynamics of protein folding: Monte Carlo simulations*, Biophys. J. **90**, 1767 (2006).
- [32] J. Mittal and R. B. Best, *Thermodynamics and kinetics of protein folding under confinement*, Proc. Natl. Acad. Sci. USA **105**, 20233 (2008).
- [33] M. Bilsel, B. Tasdizen, H. Arkin, and W. Janke, Jülich IAS Series **8**, 21 (2012).
- [34] D. Lucent, V. Vishal, V. S. Pande, *Protein folding under confinement: A role for solvent*, Proc. Natl. Acad. Sci. USA **104**, 10430 (2007).
- [35] D. T. Seaton, S. Schnabel, D. P. Landau, and M. Bachmann, *From flexible to stiff: Systematic analysis of structural phases for single semiflexible polymers*, Phys. Rev. Lett. **110**, 028103 (2013).
- [36] M. Marenz and W. Janke, *Knots as a topological order parameter for semiflexible polymers*, Phys. Rev. Lett. **116**, 128301 (2016).
- [37] J. Zierenberg, M. Marenz, and W. Janke, *Dilute semiflexible polymers with attraction: Collapse, folding and aggregation*, Polymers **8**, 333 (2016).
- [38] A. M. Ferrenberg and R. H. Swendsen, *New Monte Carlo technique for studying phase transitions*, Phys. Rev. Lett. **61**, 2635 (1988); *Optimized Monte Carlo data analysis, ibid.* **63**, 1195 (1989); S. Kumar, J. Rosenberg, D. Bouzida, R. H. Swendsen, and P. Kollman, *The weighted histogram analysis method for free-energy calculations on biomolecules. I. The method*, J. Comput. Chem. **13**, 1011 (1992).
- [39] K. Hukushima and K. Nemoto, *Exchange Monte Carlo method and application to spin glass simulations*, J. Phys. Soc. Jpn. **65**, 1604 (1996).
- [40] J. Zierenberg, M. Marenz, and W. Janke, *Scaling properties of a parallel implementation of the multicanonical algorithm*, Comput. Phys. Commun. **184**, 1155 (2013).
- [41] B. A. Berg and T. Neuhaus, *Multicanonical algorithms for first order phase transitions*, Phys. Lett. B **267**, 249 (1991); *Multicanonical ensemble: A new approach to simulate first-order phase transitions*, Phys. Rev. Lett. **68**, 9 (1992).
- [42] W. Janke, *Multicanonical simulation of the two-dimensional 7-state Potts model*, Int. J. Mod. Phys. C **03**, 1137 (1992); *Multicanonical Monte Carlo simulations*, Physica A **254**, 164 (1998).
- [43] B. Efron, *The Jackknife, the Bootstrap and other Resampling Plans* (Society for Industrial and Applied Mathematics, Philadelphia, 1982).
- [44] S. Schöbl, J. Zierenberg, and W. Janke, *Influence of lattice disorder on the structure of persistent polymer chains*, J. Phys. A: Math. Theor. **45**, 475002 (2012); S. Schöbl, S. Sturm, W. Janke, and K. Kroy, *Persistence-length renormalization of polymers in a crowded environment of hard disks*, Phys. Rev. Lett. **113**, 238302 (2014).
- [45] More specifically, DNA under typical conditions shows a persistence length of  $l_p \approx 50\text{nm}$ . Depending on the salt concentration, the thickness  $d$  of DNA varies between 2.5nm and 5nm including screened electrostatic interactions. This thickness enters in coarse-grained models as the bead size  $\sigma$ . Within the discrete worm-like chain approximation we obtain  $\kappa/k_B T \approx l_p/\sigma \approx 10 - 20$ . Our energy scale maps typical temperatures to  $k_B T \approx 1$ , such that  $\kappa \approx 10 - 20$  depending on the solution [46]. In this approximation, chains of length  $N = 28$  correspond to very short strands of about  $L = dN \approx (70 - 140)\text{nm}$  which corresponds to (210 – 420) base pairs.
- [46] B. Trefz, J. Siebert, and P. Virnau, *How molecular knots can pass through each other*, Proc. Natl. Acad. Sci. USA **111**, 7948 (2014).
- [47] T. Vogel, M. Bachmann, and W. Janke, *Freezing and collapse of flexible polymers on regular lattices in three dimensions*, Phys. Rev. E **76**, 061803 (2007).
- [48] L. Dai, C. Renner, J. Yan, and P. S. Doyle, *Coil-globule transition of a single semiflexible chain in slitlike confinement*, Sci. Rep. **5**, 18438 (2015).
- [49] M. P. Taylor, *Polymer folding in slitlike nanoconfinement*, Macromolecules **50**, 6967 (2017).
- [50] P. W. K. Rothmund, *Folding DNA to create nanoscale shapes and patterns*, Nature **440**, 7082 (2006).
- [51] N. Koga, R. Tatsumi-Koga, G. Liu, R. Xiao, T. B. Acton, G. T. Montelione, and D. Baker, *Principles for designing ideal protein structures*, Nature **491**, 222 (2012).